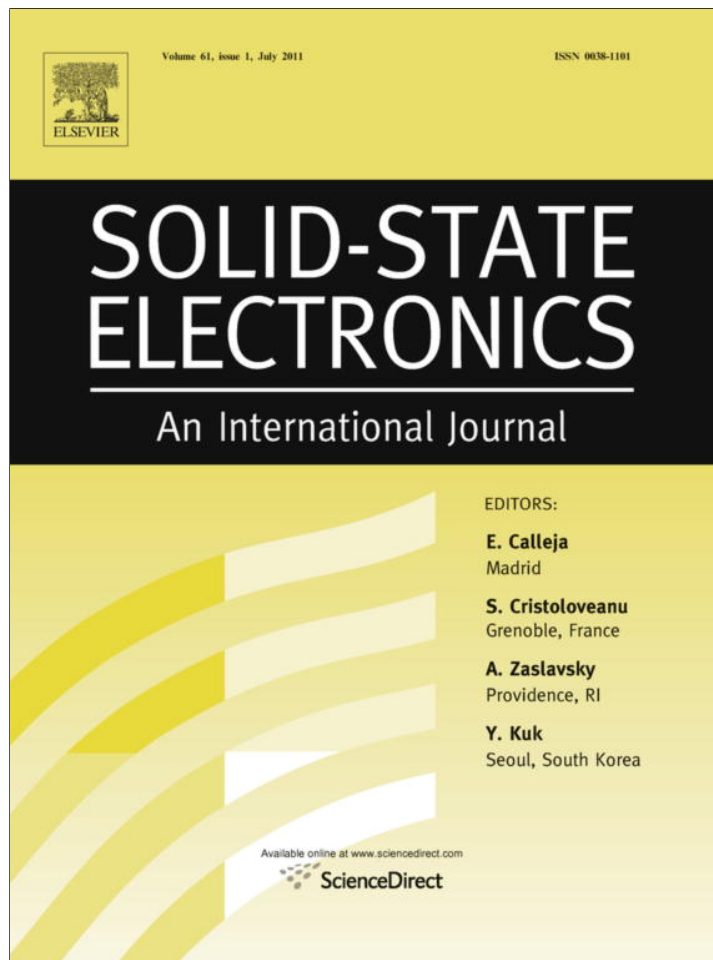


Provided for non-commercial research and education use.
Not for reproduction, distribution or commercial use.



This article appeared in a journal published by Elsevier. The attached copy is furnished to the author for internal non-commercial research and education use, including for instruction at the authors institution and sharing with colleagues.

Other uses, including reproduction and distribution, or selling or licensing copies, or posting to personal, institutional or third party websites are prohibited.

In most cases authors are permitted to post their version of the article (e.g. in Word or Tex form) to their personal website or institutional repository. Authors requiring further information regarding Elsevier's archiving and manuscript policies are encouraged to visit:

<http://www.elsevier.com/copyright>



Contents lists available at ScienceDirect

Solid-State Electronics

journal homepage: www.elsevier.com/locate/sse

Analytic expression for the Fowler–Nordheim V – I characteristic including the series resistance effect

E. Miranda^{a,*}, F. Palumbo^b^a Departament d'Enginyeria Electrònica, Universitat Autònoma de Barcelona, 08193 Bellaterra, Spain^b Consejo Nacional de Investigaciones Científicas y Técnicas – Comisión Nacional de Energía Atómica (CONICET-CNEA), Av. Gral. Paz 1499, 1650 Buenos Aires, Argentina

ARTICLE INFO

Article history:

Received 14 August 2010

Received in revised form 24 March 2011

Accepted 26 March 2011

Available online 19 April 2011

The review of this paper was arranged by Prof. S. Cristoloveanu

Keywords:

MOS

Fowler–Nordheim

Tunneling

ABSTRACT

It is shown in this communication that the Fowler–Nordheim (FN) tunneling expression for the current–voltage (I – V) characteristic can be analytically inverted so that an exact expression for the voltage–current (V – I) characteristic can be obtained. The solution of the resulting implicit equation is found using the Lambert W function, *i.e.* the solution of the transcendental equation $we^w = x$. The reported expressions are supported by experimental I – V curves measured in thin (≈ 5 nm) SiO_2 films in MOS capacitors. The analysis includes the case of a tunneling oxide with a large series resistance. For practical purposes, a closed-form expression for W based on a Padé-type approximation is also provided.

© 2011 Elsevier Ltd. All rights reserved.

1. Introduction

The reduction of the gate dielectric thickness in metal–oxide–semiconductor (MOS) structures leads to an exponential increase of the leakage current flowing through the device. In turn, this large current increase is the origin of a significant deviation from the “ideal” conduction characteristic because of the series resistance effect [1–4]. Contrary to what happens to a diode with a series resistance [5–7], to the best of our knowledge, no analytical solution for the Fowler–Nordheim (FN) tunneling characteristic with such additional feature has been reported to the date. The presence of a series resistance in a MOS device has important consequences for the reliability analysis of ultrathin oxides since it affects the breakdown statistics both in the case of voltage/current ramp tests [1] as well as for constant electrical stress [2]. As it is well known, for voltages larger than ≈ 4 V, the current in thin SiO_2 films is mainly due to tunneling through a triangular potential barrier whose shape is dictated by the cathode barrier height and the oxide field [8]. The same is applicable to any other dielectric operating in such regime. The FN model arises from considering the Wentzel–Kramers–Brillouin (WKB) approximation for calculating the transmission probability through a triangular barrier so that the resulting expression is only able to capture the average behavior of the current. More elaborated treatments based on solv-

ing the Schrödinger equation reveal that the current oscillates around the average value because of the partial reflection of the electron wave functions at the anode interface [9]. The analysis of these oscillations is out of the scope of this communication so that they will not be discussed further. It is worth mentioning that even though this report is specifically concerned with MOS devices, the impact of the series resistance on the FN current has been investigated in connection with carbon nanotubes used as electron field emitters as well [10–12].

In this work, we report an analytical expression for the FN characteristic in which the current rather than the voltage plays the role of the independent variable. In this way, we are able to represent by means of a transformation that involves the Lambert W function [13] the exact V – I curve or equivalently, by a simple exchange of the plotting axes, the I – V curve.

2. The samples

In this study, MOS capacitors with oxide thickness $t_{\text{ox}} = 4.9$ nm and square areas S ranging from 10^{-5} to 10^{-2} cm^2 were used. The substrate is p-type (1 0 0) Si with a doping concentration of about 10^{15} cm^{-3} . The oxidation was carried out in a dry N_2/O_2 atmosphere at 800 °C. Poly-Si gates 350 nm-thick were deposited by LPCVD and subsequently n^+ doped by POCl_3 diffusion at 900 °C. Metal contact pads were defined on a 400 nm-thick field oxide. Measurements were performed at room temperature and dark conditions. Negative voltages were applied to the gate with the

* Corresponding author.

E-mail address: enrique.miranda@uab.es (E. Miranda).

substrate contact grounded. The use of different areas allowed us to test devices with different series resistances [4] without introducing any additional resistive component in the characterization circuit.

3. Parameters extraction and model equations

According to the FN model [8,9], the current density $J = I/S$ that flows through a thin dielectric layer when a field F is applied reads:

$$J(F) = AF^2 \exp\left(-\frac{B}{F}\right) \quad (1)$$

where $A = \frac{mq^3}{8\pi\hbar m^* \Phi}$, $B = \frac{8\pi\sqrt{2m^*}\Phi^{3/2}}{3\hbar q}$, m the electron mass, m^* the effective electron mass in the insulator, \hbar the Planck's constant, q the electron charge, and Φ the cathode barrier height. Fig. 1 shows typical I - V characteristics for the available set of devices. With the substitution $F = B/2\gamma$, Eq. (1) reads $ye^y = \frac{1}{2}\left(\frac{AB^2}{J}\right)^{1/2}$, so that using the Lambert W function [13], i.e. the solution of the equation $W(x)e^{W(x)} = x$, it is obtained:

$$F(J) = \frac{B}{2W\left[\frac{1}{2}\left(\frac{AB^2}{J}\right)^{1/2}\right]} \quad (2)$$

In case of a MOS barrier with a resistance R in series, the oxide field is given by the expression $F = (V - \Delta V - SJ.R)/t_{ox}$, where V is the applied voltage and ΔV any possible correction due to the flatband voltage and potential drops at the electrodes. Notice that, with the inclusion of R , F depends on the current flowing through the device so that Eq. (1) is an implicit function of J . Even though, in general, ΔV is a function of V , for the sake of simplicity we assume $\Delta V = 1.2$ V, which represents an average value for different oxide thicknesses and technologies in accumulation conditions, including polysilicon depletion [14]. In order to simulate the I - V characteristics it is necessary first to have a well-defined set of model parameters. Following [15], R , A , and B can be accurately determined from the linearization of the FN plot. Fig. 2 shows the effect of varying R on the FN plot linear correlation coefficient (LCC). In particular, for the device with area $S = 9.6 \times 10^{-3}$ cm², $R = 952.3$ Ω , $A = 1.78 \times 10^{-7}$ A/V² and $B = 238$ MV/cm are found. Assuming $m^* = 0.5 m$ [16], we found $\phi = 2.92$ eV, which is within the common accepted range for the cathode barrier height in these structures [17]. The oscillatory behavior of the current is clearly visible, especially in

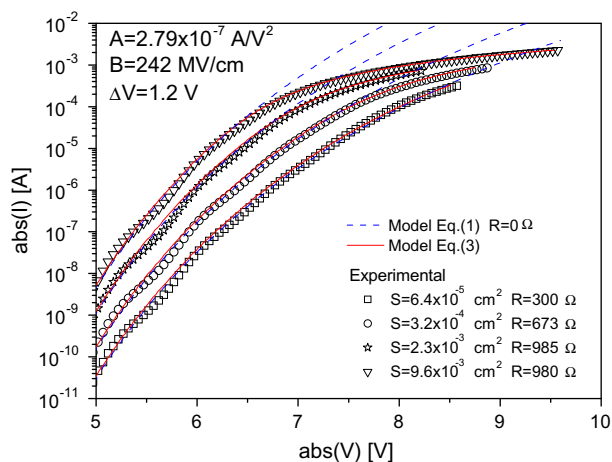


Fig. 1. Current–voltage characteristics for different gate areas ranging from 10^{-5} to 10^{-3} cm². The symbols correspond to the experimental data whereas the solid (red) and dashed (blue) lines correspond to simulated I - V curves. (For interpretation of the references to color in this figure legend, the reader is referred to the web version of this article.)

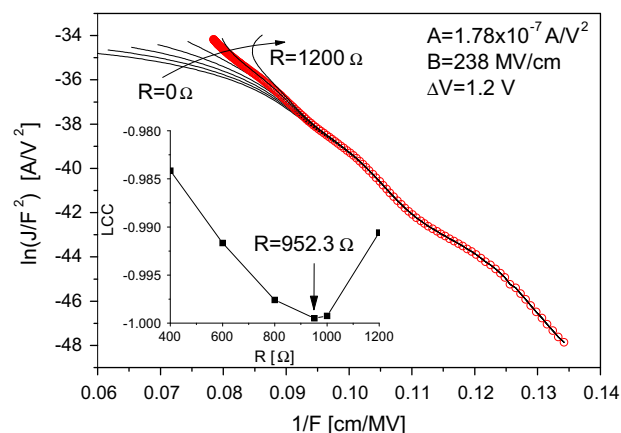


Fig. 2. Fowler–Nordheim plots for the data corresponding to the sample with area $S = 9.6 \times 10^{-3}$ cm² shown in Fig. 1. The inset shows the linear correlation coefficient (LCC) associated with these curves as a function of R . The minimum is found for $R = 952.3$ Ω (red symbols). (For interpretation of the references to color in this figure legend, the reader is referred to the web version of this article.)

the low field FN region ($F < 10$ MV/cm). This part of the curve is practically not affected by the series resistance value. Since we are interested in modeling a set of characteristics measured on devices with different gate areas, instead of analyzing isolated I - V curves one by one, we minimize the LCC associated with the full I - V data vector (four curves) but keeping R independent for each individual curve. The outcome of this optimization and fitting process is shown in Fig. 3. In this case $A = 2.79 \times 10^{-7}$ A/V² and $B = 242$ MV/cm are found, which are slightly different from the previous values because of the global optimization process. Notice that, assuming $m^* = 0.5 m$ and $\phi = 2.92$ eV, $A = 2.63 \times 10^{-7}$ A/V² is calculated from the FN theory, which is in close agreement with the experimental value of A referred above. Next, using Eq. (2) and the definition of the oxide field, we obtain:

$$V = \Delta V + SJR + \frac{Bt_{ox}}{2} \left\{ W \left[\frac{1}{2} \left(\frac{AB^2}{J} \right)^{1/2} \right] \right\}^{-1} \quad (3)$$

which is the theoretical expression for the V - J characteristic we were looking for. In Fig. 1, fitting results obtained with Eq. (3) (red solid line) and with the standard FN model Eq. (1) (blue dashed

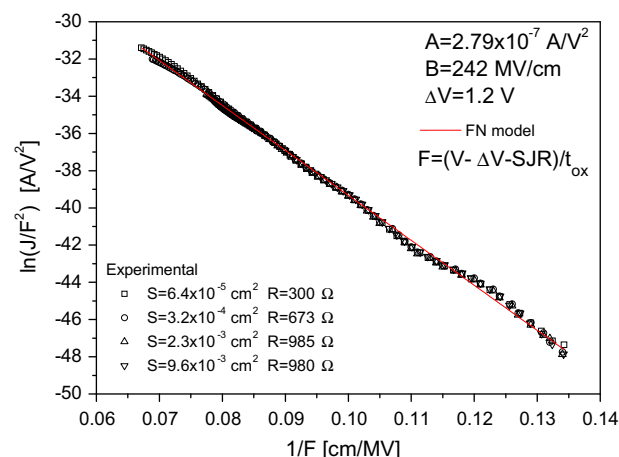


Fig. 3. Fowler–Nordheim plots after global optimization for samples with different areas. The red solid line shows the best fitting result associated with the full I - V data vector (four curves). (For interpretation of the references to color in this figure legend, the reader is referred to the web version of this article.)

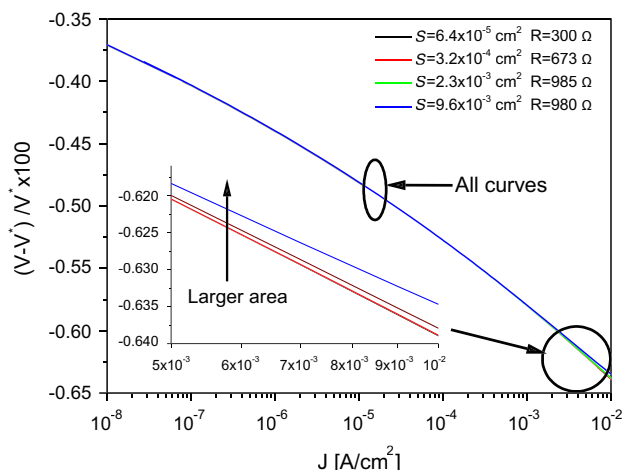


Fig. 4. Relative error in the gate voltage $(V-V^*)/V^*$ as a function of the current density J . V is calculated using Eq. (3) and the value of the Lambert W function given by the Padé approximation Eq. (4). V^* is the value of the Lambert W function provided by MATLAB.

line) are compared. As expected the agreement is total in the low field region and the deviations become evident as the potential drop across R cannot longer be neglected.

To go farther, a crucial point that needs to be discussed in connection with the Lambert W function is what kind of approximation should be used to compute it. In this regard, let us point out that Eq. (3) is considered an exact result in the sense that W can be numerically determined within the required precision. Many commercial software packages like MATLAB or MATHEMATICA provide efficient solutions to this problem. However, a major question with the analytic treatment of this function is that its Taylor series oscillates between ever larger positive and negative values becoming useless for practical purposes [18]. An alternative method other than a series expansion is therefore imperatively required. In [19], it was shown that a practical formula to compute W is given by the expression:

$$W(x) \approx \ln(1+x) \left\{ 1 - \frac{\ln[1 + \ln(1+x)]}{2 + \ln(1+x)} \right\} \quad (4)$$

which is based on a Padé-type approximation. Other expressions can also be found in literature [13–18] but are more complicated. The solid lines in Fig. 1 were calculated using Eq. (4). Finally, in order to show that Eq. (4) is accurately enough, Fig. 4 illustrates the error in the gate voltage given by Eq. (3) calculated using Eq. (4) and the results provided by MATLAB for the Lambert W function. The agreement is excellent within the considered experimental voltage/current window and the error is only slightly dependent on the series resistance values (see Fig. 4's inset). In any case, the error is always less than 0.65% in the gate voltage for any given current level.

4. Conclusion

A closed-form expression for the Fowler–Nordheim tunneling characteristic (V – I) in MOS devices including the series resistance effect was reported. In order to fit the experimental data we have utilized a simple yet accurate method for extracting the parameters associated with this conduction mechanism based on the linearization of the Fowler–Nordheim plot. An approximate expression for the Lambert W function based on a Padé-type approximation was also provided.

Acknowledgements

F.P. and E.M. gratefully acknowledge the economical support from the International Center of Theoretical Physics (ICTP), Trieste, Italy under the Associate Scheme and Visitor Scientist Program, respectively. This work has been partially supported by PICT05-38255 and PICT07-01143 ANPCyT, Argentina and TEC2009-09350, Spain.

References

- [1] Monroe D, Swanson S. Complete method for E_{bd} correction by series resistance characterization. Integr Reliab Workshop Final Rep, IEEE Int 1998:33.
- [2] Roy D, Bruyere S, Vincent E, Monsieur F. Series resistance and oxide thickness spread influence on Weibull breakdown distribution: new experimental correction for reliability projection improvement. Mic Rel 2002;42:1497.
- [3] Hu D. Effects of the series resistance on Fowler–Nordheim tunneling oscillations. Solid-State Electron 1996;41:513.
- [4] Pio F. Sheet resistance and layout effects in accelerated tests for dielectric reliability evaluation. Microelectron J 1996;27:675.
- [5] Fjeldly T, Moon B, Shur M. Approximate analytical solution of generalized diode equation. IEEE Trans Electron Dev 1991;ED-38:1976–7.
- [6] Banwell T, Jayakumar A. Exact analytical solution for the current flow through diode with series resistances. Electron Lett 2000;36:291–2.
- [7] Ortiz-Conde A, García-Sánchez F, Muci J. Exact analytical solutions of the forward non-ideal diode equation with series and shunt parasitic resistances. Solid-State Electron 2000;44:1861.
- [8] Lenzlinger F, Snow E. Fowler–Nordheim tunneling into thermally grown SiO_2 . J Appl Phys 1969;40:278.
- [9] Maserjian J, Zamani N. Behavior of the Si/SiO₂ interface observed by Fowler–Nordheim tunneling. J Appl Phys 1982;53:559.
- [10] Dean K, Chalamala B. Current saturation mechanisms in carbon nanotube field emitters. Appl Phys Lett 2000;76:375.
- [11] Cui J, Robertson J. Control of field emission current of individual sites by a local resistor. J Vac Sci Technol 2002;B 20:19.
- [12] Bonard J, Klinke C, Dean K, Coll B. Degradation and failure of carbon nanotube field emitters. Phys Rev 2003;B 67:115406.
- [13] Corless R, Gonnet G, Hare D, Jeffrey D, Knuth D. On the Lambert W Function. Adv Comput Math 1996;5:329.
- [14] Schuegraf K, Hu C. Hole injection SiO_2 breakdown model for very low voltage lifetime extrapolation. IEEE Trans Electron Dev 1994;41:761.
- [15] Miranda E. Method for extracting series resistance in MOS devices using Fowler–Nordheim plot. Elec Lett 2004;40:1153.
- [16] Weinberg Z. On tunneling in metal–oxide–silicon structures. J Appl Phys 1982;53:5052.
- [17] Hadjadj A, Salace G, Petit C. Fowler–Nordheim conduction in polysilicon (n+)–oxide–silicon (p) structures: Limit of the classical treatment in the barrier height determination. J Appl Phys 2001;89:7994.
- [18] Weisstein E. Lambert W-function from MathWorld, A Wolfram Web Resource. <<http://www.mathworld.wolfram.com/LambertW-Function.html>>.
- [19] Wintzki S. Uniform approximations for transcendental functions. Lecture notes in computer science. Springer; 2003.